

PROPERTIES AND RELATED PERFORMANCE OF C/C COMPOSITES: II. COEFFICIENT OF FRICTION

Soydan Ozcan^{a,b}, Katarzyna Peszynska-Bialczyk^b, Dale E. Wittmer^a, Peter Filip^{a,b}

a. Mechanical Engineering and Energy Processes, Southern Illinois University, Carbondale, IL, USA

b. Center for Advanced Friction Studies, Southern Illinois University, Carbondale, 62901, USA

ABSTRACT

The influence of heat treatment temperature on frictional performance of C/C aircraft brake composite was studied. C/C composites were heat treated at temperatures of 1800°C, 2100°C and 2400°C, respectively. The coefficient of friction (COF) was obtained from subscale aircraft brake dynamometer tests performed at 50% relative humidity level and various landing conditions. Real time CO₂ release during the friction process was measured using a mass spectroscopy. After each friction test, the roughness of the friction surfaces was measured using stylus surface profilometry. Structural changes of the friction debris collected were characterized by X-ray diffraction. The COF exhibited specific transitions during the 100 % normal landing energy simulations for all three samples. This COF transition was attributed to the oxidation of composites when they reached the critical temperature. The highest friction surface roughness was always detected for C/C samples heat treated at 2400°C and these materials exhibited abrasive wear. The differences in frictional behavior were attributed to the microstructural changes related to the applied heat treatment.

INTRODUCTION

The use of carbon fiber reinforced carbon (C/C) composite in high temperature braking and structural applications has become increasingly common. C/C composites exhibit excellent mechanical and thermal properties [1-3]. Hardly any material can match the high specific strength, toughness, low thermal expansion and its ability to retain these properties at high temperatures. Nonetheless, the ever-competitive performance-driven market demands better C/C materials that can outperform their predecessors in terms of cost and performance [4-6].

This paper summarizes the data obtained from the subscale aircraft dynamometer testing and related properties of C/C composites brake materials heat treated at different temperatures. The objective is to compare the coefficient of friction during simulated landings and show the influence of C/C properties on frictional performance.

EXPERIMENTAL PROCEDURE

Three directional non-woven needled felt PAN fiber reinforced CVI matrix commercial composites were used in this research. The non-heat treated samples (NHT) were kindly provided by Honeywell Aircraft Landing System. The samples were heat-treated at the Center for Advanced Friction Studies laboratories using a graphitization furnace (Model: TP-4X10-G-G-D64A-A-27, Centorr Associates Inc). The heat treatment was performed in an argon atmosphere for 1 hour at temperatures of 1800°C, 2100°C and 2400°C, respectively (Table 1).

Table I. Sample notifications and corresponding heat treatment temperatures.

Sample name	Heat treatment temperature (C°)
NHT	Non-heat-treated
CC18	1800
CC21	2100
CC24	2400

Friction and wear tests were performed using the Link Engineering sub-scale aircraft brake dynamometer (Model 2076, Plymouth, MI, USA) with C/C discs scaled down in by energy/mass ratio. The nominal outer and inner diameters of the ring specimens were 92.25 mm (3.75”) and 69.85mm (2.75”), respectively. The schematic diagram of the computer controlled subscale aircraft dynamometer equipped with environmental chamber is shown in figure 1.

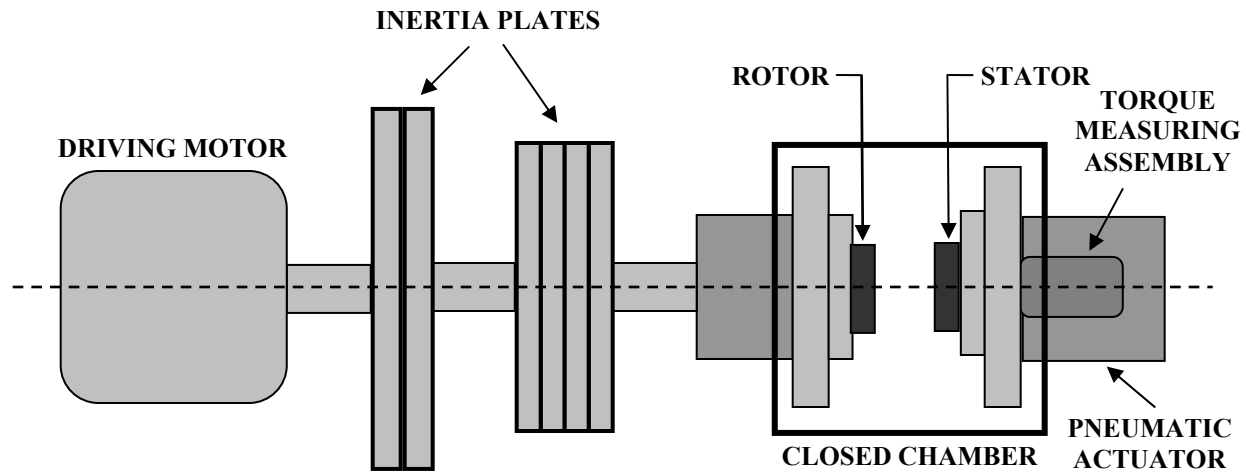


Figure 1. Schematic diagram of subscale aircraft dynamometer used in research.

The friction tests were simulated at 12.5, 25, 50 and 100% of normal landing energy (NLE). For each simulation of landing three taxis performed at 4.5% NLE followed by one landing stop was repeated 50 times for each energy condition (200 braking events). The initial temperature of each test stop was set up on $T_0 = 50\text{ }^\circ\text{C}$ ($120\text{ }^\circ\text{F}$) and the applied normal force ramp rate dF/dt was set up on the value of 1780 N/s (400 lb/s). The coefficient of friction, temperature, torque, decelerating speed and normal force is measured in real time. The relative humidity level (50 %) was maintained with a humidity control system within a 1% of the desired value. The subscale aircraft brake dynamometer was operated in constant torque mode (2.041 kgf-m), the normal force varied in response to the current coefficient of friction. For the period of the braking process, a number of parameters such as stop time: (7 to 34 sec), contact pressure (0.08 MPa to 0.35 MPa) and speed (202.8 km/h) were controlled.

A mass spectrometer (Hewlett Packard 5970) was coupled with the environmental chamber of the dynamometer system and the gaseous products released during braking were continuously monitored along with atmospheric Argon (Ar) which served as a convenient reference standard for CO_2 analysis. Normalized results from the MS (CO_2/Ar ratio) were correlated to wear of the C/C material measured as mass loss.

Microstructure of C/C composites was characterized using a Nikon Microphot-FX polarized light microscope (PLM). Three specimens corresponding to different directions (X: tangential, Y: radial, Z: through the thickness of brake disc) were prepared from each of the four composites. They were mounted in epoxy resin ground and polished. Different diamond polishing slurries with the grain size from $6\mu\text{m}$ down to $0.25\mu\text{m}$ were used, subsequently.

The XRD studies of samples subjected to different HTT were performed using the Rigaku D-MAX B X-Ray diffractometer. The samples were pulverized, and the powder was mixed 50% by weight with 99.99% pure well annealed Ni with a particle size of $10\mu\text{m}$. Ni served as an internal standard for X-ray diffraction patterns. A glass slide was prepared with a petroleum jelly glaze, and the mixed powder was dusted on the slide to prevent preferred orientation. $\text{Cu}_{K\alpha}$ radiation ($\lambda=1.54056\text{ \AA}$, $V = 20\text{ kVA}$, $I = 30\text{ mA}$, Ni filtered, 2-theta at $0.6^\circ/\text{min}$) was used. The maximum peak for a (111) plane of Ni (PDF Card 04-0850) with a d-spacing of 2.0340 \AA was used as the standard in this analysis. The XRD results were obtained for each sample between 20 and 50° . The peak search program was then used to analyze the (002) peaks and find the d-spacing and the crystallite size for the carbon.

RESULTS AND DISCUSSIONS

The polarized light microscopy (PLM) images of characteristic microstructure of the investigated non-heat treated composite are shown in Fig. 2. The PAN fibers with turbostratic microstructure are surrounded by a rough laminar CVI carbon with an average extinction angle $Ae = 20^\circ$. Since the fibers are quite close to each other with a small deposition thickness in the PAN carbon fiber bundle regions, Deposition thickness of CVI carbon is quite large in the vicinity of large pores (up to $15\mu\text{m}$). Larger microporosity formed dominantly between the fiber bundles (Fig. 2a), whereas the interior of the fiber bundle regions are typified by the presence of smaller pores (Fig. 2).

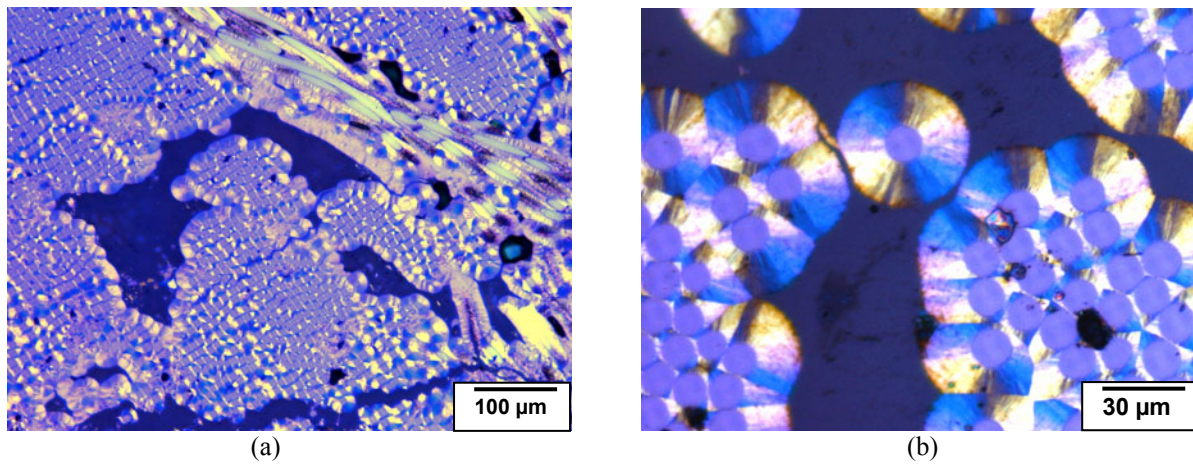


Figure 2. Characteristic low (a) and high (a) magnification polarized light microscopy images

The X-ray diffraction results for the bulk materials are given in figures 3. The XRD results for the NHT sample reveal that this peak is not symmetric and is believed to contain contributions from both the fiber and the CVI matrix. The XRD results were similar for the CC18 and the NHT samples evidencing that the heat treatment temperature of 1800°C is too low to cause changes in the microstructure of the NHT samples. However, the diffraction peaks become sharper with increasing heat treatment temperature and also shift to higher 2-theta values, which is an indication of increased crystallinity and decreased interplanar (002) d-spacing.

The interplanar spacings (d_{002}) and crystallite sizes of samples are summarized in Table II. With increased heat treatment temperature, the interplanar d-spacing decreased gradually from 3.4239 Å to 3.4075 Å, and the crystallite size increased from 103 Å to 193 Å, which are both evidence of increased organization towards a more graphitic structure. As expected, this composite do not contain graphitic structures however, a better organized and coherent domains of carbon grow with increased heat treatment temperature. When compared to the polarized light microscopy results, it is obvious that all microstructures obtained after different heat treatment temperatures contained at least two different types of carbon. A less organized fiber and a better organized CVI matrix carbon create a compound (002) peak.

Table 1. Crystallite size and interplanar spacing (d_{002}) for heat treated C/C composites.

Sample Identification	Crystallite Size (Å)	Interplanar spacing (Å)
NHT	103	3.4239
CC18	106	3.4177
CC21	161	3.4177
CC24	193	3.4075

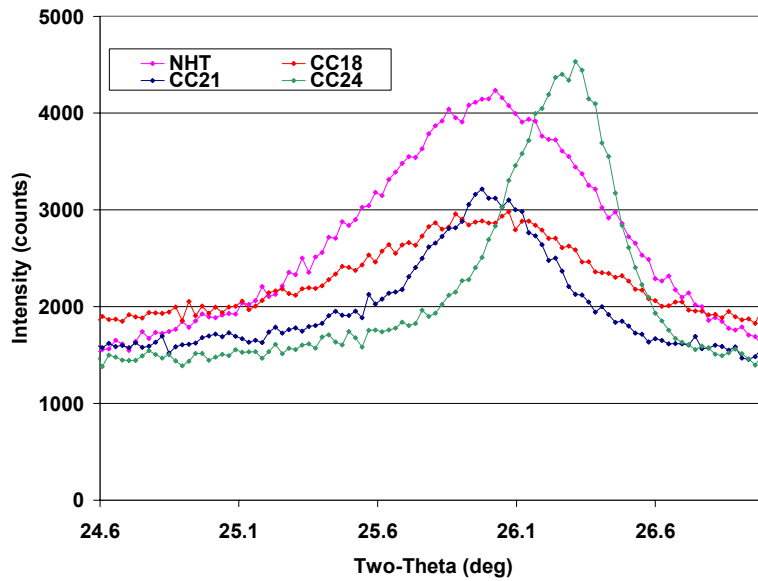


Figure 3. 002 Peak of carbon observed in the X-Ray diffraction pattern of studied C/C composite subjected to different final heat treatment temperatures.

XRD patterns of collected wear debris during the dynamometer testing at various conditions for all heat treated samples are given in figure 4. Identical experimental procedure was applied to the bulk and debris using the same X-Ray diffraction equipment. Even though a strong (002) carbon peak is obvious for the bulk composite (shown in figure 3), no visible (002) peak is observed in the XRD pattern of the wear debris indicating the amorphous microstructure of the collected wear debris. This shows that the applied force during the friction damaged the crystalline microstructure of wear debris.

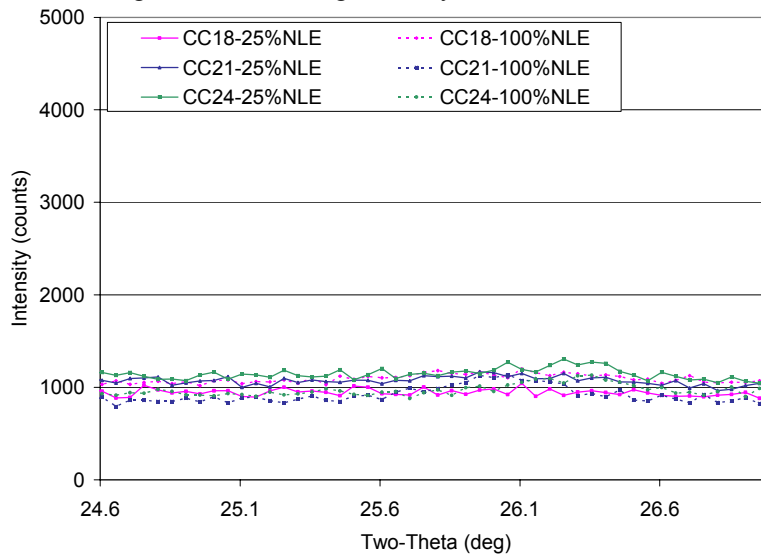


Figure 4. X-Ray diffraction patterns of wear debris collected during aircraft braking tests performed at 50%relative humidity and 25 or 100 % normal landing energy simulations.

Roughness (Ra) of friction surfaces after different simulated landings is plotted in figure 5. Roughness of friction surfaces increased with increased heat treatment temperature of the C/C composites. However, no a simple correlation can be established between the coefficient of friction and the friction surface roughness.

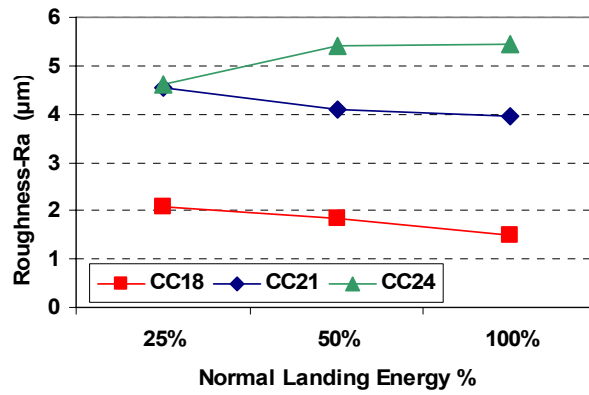


Figure 5. Roughness data (Ra) after the friction test performed at 50% relative humidity conditions and 25, 50, 100%NLE.

Figure 6 shows the size of integrated areas under CO₂/Ar signals detected by MS coupled with the dynamometer. CO₂ release was attributed to the oxidation of the C/C composite materials during the friction process. The total amount of released CO₂ varied depending on the final heat treatment temperature and simulated landing conditions. For CC24, CO₂ release is almost identical at different simulated landing energy conditions. However, in the case of CC18, the CO₂ release was considerably different when 25% and 100%NLE conditions compared. This indicates that heat treated materials with better ordered microstructure (larger crystallite size, change from turbostratic to graphite-like carbon) are more resistant to oxidative process.

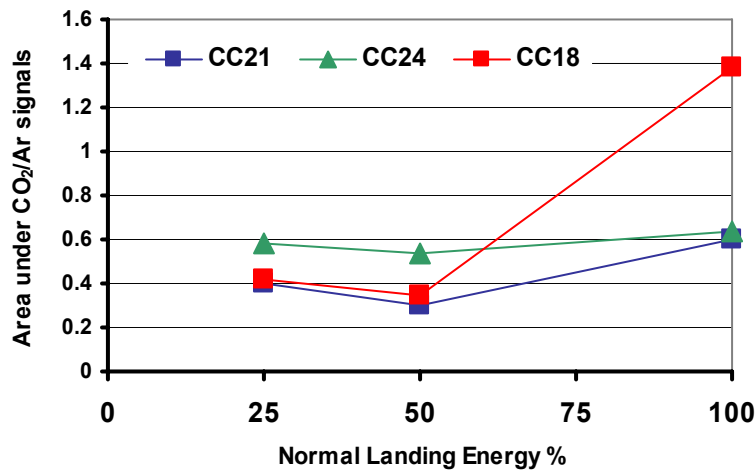


Figure 6. The cumulative CO₂/Ar ratio (total area under the peaks) for heat treated materials detected at 50%RH and different dynamometer NLE conditions.

Average coefficient of friction of investigated C/C composites during individual stops is shown in figure 7. Up to 50% NLE, the coefficient of friction found to be increased with the increased heat treatment temperatures of the C/C composites. However, CC18 exhibited the highest coefficient of friction at 100%NLE. Importantly the coefficient of friction was high, when the amount of CO₂ release was high. That means that oxidation itself (increased CO₂ content) does not necessarily leads to lubrication as stated by other authors [7,8]. At 100% NLE simulations, the amount of released CO₂ was higher than that of at 50 and 25%NLE for each composite and the detected coefficient of friction was higher than the lower energy conditions for each composite. Moreover, in the case of 25 % and 50 % NLE conditions, released CO₂ during test was the highest for the CC24 and also detected coefficient of friction during simulated landing stops at corresponding conditions was the highest.

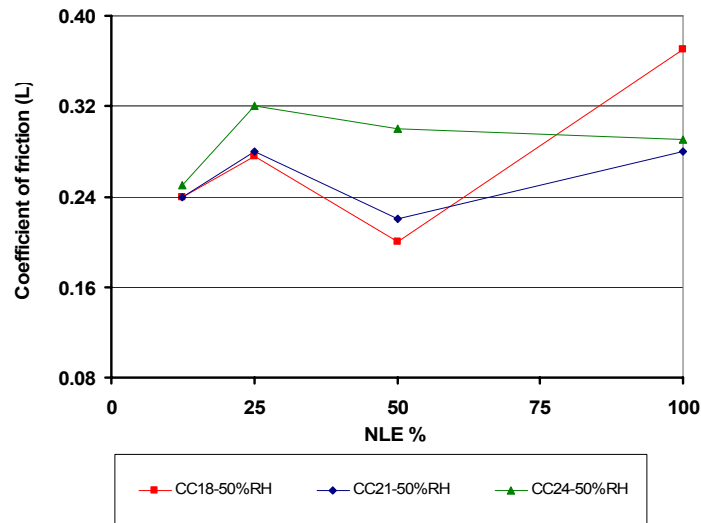


Figure 7. The average coefficient of friction (calculated from 200 experiments) of simulated landing stops at 50% RH and various landing energy conditions.

Characteristic development of the coefficient of friction during individual stops performed at 25% and 100%NLE conditions are given in figure 8. At 25% NLE simulation, the coefficient of friction remains relatively stable and a gradual decrease is detected towards the end of landing stop. The measured temperature is similar for all samples subjected to different heat treatment temperature at 25% NLE simulation. At 100% NLE, however, Surface temperature of CC18 is higher compared to other two tested composites. In addition, CC18 typically exhibited noisy stops at 100% NLE and considerable transition in friction was observed 2 seconds after the engagement of the discs. A smaller transition was observed for CC21 at 100%NLE simulation. Compared to CC18 the transition detected for CC21 occurred several seconds later. The higher the heat treatment temperature, the better ordered is the carbon in C/C composites and this results in higher thermal conductivity. The delay of transition at 100% NLE with an increasing heat treatment temperature of the C/C composites is obviously related to the better thermal properties of the samples. Since a high thermally conductive C/C composite is able to better transfer the friction generated heat from the friction surface.

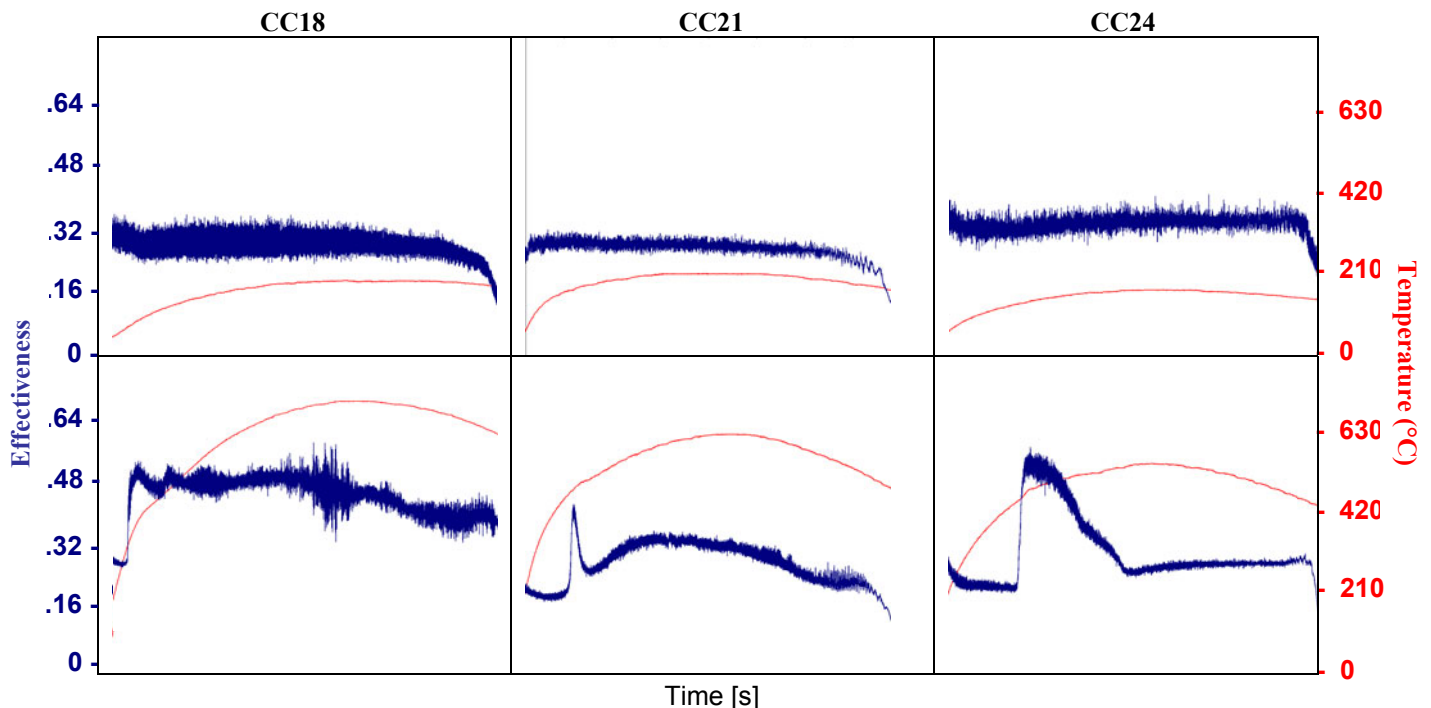


Figure 8. Characteristic individual stops of CC18, CC21 and CC24 at 25%NLE (first row) and 100%NLE (second row) at 50% relative humidity level (red line indicates the temperature (C°) and blue line is coefficient of friction (unitless)).

CONCLUSIONS

C/C composites with an architecture consisting of a three dimensional non-woven PAN fiber in a CVI matrix were heat treated between the temperature of 1800°C and 2400°C. XRD results showed an increase in carbon crystallite size and a decrease of interplanar spacing as a function of increased heat treatment temperature. A less organized fiber and a more organized CVI matrix create a compound (002) peak consisting of diffraction contributions from both. A higher friction surface roughness was always detected for the samples heat treated at 2400°C. Coefficient of friction was always detected high in the simulated landing stops when the amount of CO₂ release is high.

ACKNOWLEDGEMENTS

This research was sponsored by state of Illinois and the consortium of 12 industrial partners of Center for Advanced Friction Studies (<http://frictioncenter.engr.siu.edu>). The authors would like to thank to Mr. Poh Wah Lee for his assistance in dynamometer testing.

REFERENCES

1. E.Fritzer, L.M. Monacha. Carbon Reinforcements and Carbon/Carbon Composites, Springer-Verlag Berlin Heidelberg New York (1998)
2. E.Fritzer, L.M. Monacha. Carbon Reinforcements and Carbon/Carbon Composites, Springer-Verlag Berlin Heidelberg New York (1998)
3. G. Savage, Carbon-Carbon Composites. Royal Society of Chemistry, Cambridge, U.K, 1993
4. S. Ozcan, M. Kroska, P. Filip Frictional performance and local properties of C/C composites Ceramic Engineering and Science Proceedings, 29th International Conference on Advanced Ceramics and Composites, 26, pp. 127-138, (2005).
5. S. Ozcan and P. Filip, Microstructure and wear mechanisms in C/C composites, Wear, 259, pp.642-650 (2005),.
6. S. Ozcan and P. Filip, Microscopic Study of Cracking and Wear Mechanisms in 2D randomly chopped and 3D Non-woven C/C Composites. Extended Abstract-International Conference on Carbon at Brown University, 11-16 July 2004.
7. R. F. Deacon and J. F. Goodman, "Lubrication by Lamellar Solids," Proc. R. Soc. London, Ser. A, 243, pp.464-81 (1958).
8. B.K. Yen, Influence of water vapor and oxygen on the tribology of carbon materials with a sp² valance configuration, Wear, 192, pp. 208-215, (1996)